

Surprises from a Simple Material—The Structure and Properties of Nickel Cyanide**

Simon J. Hibble,* Ann M. Chippindale,* Alexander H. Pohl, and Alex C. Hannon

Compounds that can be viewed as offspring of a $\text{Ni}(\text{CN})_2$ parent have long been known and many are of exceptional interest. For example, the first inclusion compound, Hofmann's benzene clathrate $[\text{Ni}(\text{CN})_4\text{Ni}(\text{NH}_3)_2] \cdot 2\text{C}_6\text{H}_6$ discovered in 1897,^[1] is the basis of very modern phase-separation chemistry employing open-framework zeolite-like compounds based on nickel-cyanide networks.^[2] It was therefore initially surprising to find that the structure of $\text{Ni}(\text{CN})_2$ itself remained unknown, especially as any chemist would be almost certain that it would be a layered structure containing sheets formed from vertex-sharing square-planar $\{\text{Ni}(\text{CN})_4\}$ units. However, although $\text{Ni}(\text{CN})_2$ can easily be prepared by dehydration of nickel-cyanide hydrates^[3] and ammoniates,^[4] it is a highly disordered crystalline solid, as is revealed by its powder X-ray diffraction (XRD) pattern (Figure 1). Never-

theless, for such a "simple" compound, it might be expected that, as in the cases of $\text{Mn}(\text{CN})_2$ ^[5] and high-temperature CuCN ,^[6] the basic structure would have been solved using this information. Indeed a superficially plausible model built from square-planar $\{\text{Ni}(\text{CN})_4\}$ units linked to form sheets was proposed by Vegas et al.^[4] However, closer inspection of their model shows it contains implausibly short non-bonded contacts between carbon and nitrogen atoms.

Herein we report for the first time the detailed structure of $\text{Ni}(\text{CN})_2$. We have used a combination of powder X-ray and total neutron diffraction to yield accurate interatomic distances and give the stacking sequence of the sheets. We contrast the bonding of the cyanide group to nickel in $\text{Ni}(\text{CN})_2$ and in the related compound $\text{Ni}(\text{CN})_2 \cdot 3/2\text{H}_2\text{O}$ ($3/2\text{D}_2\text{O}$ for neutron diffraction), and we discuss the 2D negative thermal expansion (NTE) in $\text{Ni}(\text{CN})_2$.

Powder XRD patterns of anhydrous nickel cyanide^[7] were collected at 100 K (Figure 1) and 298 K. The patterns contain a mixture of sharp and broad reflections, suggesting that the material is highly disordered. These features, together with the rather unusual and variable peak shapes, may explain why previous attempts to solve the structure have not been successful. The temperature-dependent behavior of the sharp reflections revealed two different classes, and provided the key to indexing the powder patterns. Reflections of the type $hk0$ moved to higher 2θ values (smaller d -spacings) on warming the sample from 100 to 298 K, but the $00l$ reflections moved in the opposite sense. These observations confirmed our suspicion that $\text{Ni}(\text{CN})_2$ would show 2D NTE was correct. The fact that the hkl reflections are broad suggests that there are a large number of stacking faults present. To index all the observed reflections, a lattice parameter c that is four times the interlayer spacing is needed, resulting in a tetragonal unit cell ($a = 4.8632(4)$ and $c = 12.636(2)$ Å (100 K) and $a = 4.8570(4)$ and $c = 12.801(3)$ Å (298 K)). Assuming that the Ni–C and Ni–N distances are equal (this assumption is shown to be correct below), and that carbon and nitrogen are indistinguishable, we were able to construct a structural model in $P4_2/mmc$ that generated satisfactory C/N-to-C/N non-bonded contacts with none shorter than 3.4 Å (Figure 2).^[8] The presence of stacking faults and the resulting line broadening precluded the use of conventional Rietveld methods for structural model refinement.

To obtain further structural information for $\text{Ni}(\text{CN})_2$, total neutron diffraction data^[9] were collected at 10 and 300 K and analyzed to produce the total pair correlation function, $T(r)_{\text{exp}}$ (Figure 3). Maxima in $T(r)$ correspond to frequently occurring interatomic distances in the compound, and, at low r , can often be ascribed to "chemical bonds".^[10] The peak at 1.15 Å, for example, corresponds to the $\text{C}\equiv\text{N}$ bond. It must be

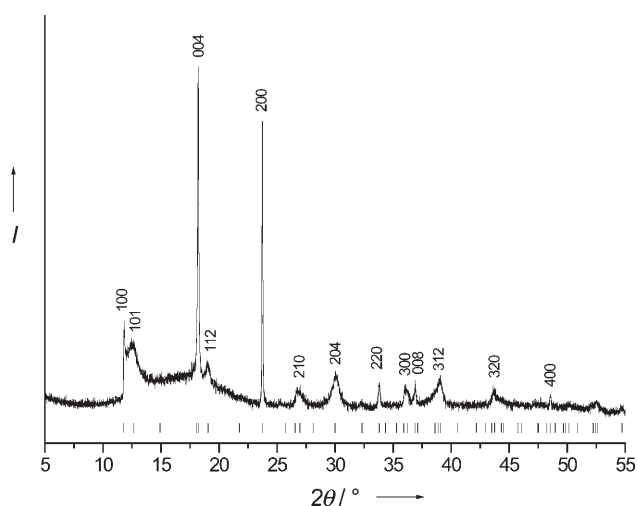


Figure 1. Powder XRD pattern of $\text{Ni}(\text{CN})_2$ at 100 K ($\lambda = 1.00$ Å).

[*] Dr. S. J. Hibble, Dr. A. M. Chippindale, A. H. Pohl
Department of Chemistry
University of Reading
Whiteknights, Reading, Berks RG6 6AD (UK)
Fax: (+44) 118-378-6331
E-mail: s.j.hibble@rdg.ac.uk
a.m.chippindale@rdg.ac.uk

Prof. A. C. Hannon
ISIS Facility
Rutherford Appleton Laboratory
Chilton, Didcot, Oxon OX11 0QX (UK)

[**] The authors acknowledge financial support from the EPSRC (Research Studentship for A.H.P.) and the Leverhulme Trust (Research Fellowship for A.M.C.).

Supporting information for this article is available on the WWW under <http://www.angewandte.org> or from the author.

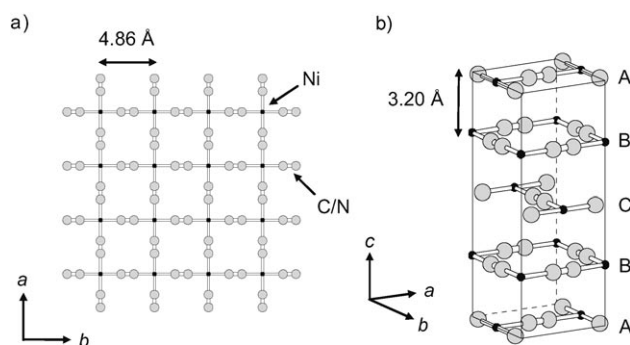


Figure 2. Structure of $\text{Ni}(\text{CN})_2$ showing a) one layer of vertex-sharing $\text{Ni}(\text{CN})_4$ units with a $\text{Ni}-\text{C}\equiv\text{N}-\text{Ni}$ distance of 4.86 Å and b) ABCBA stacking of the layers within the unit cell leading to a layer repeat distance of 12.80 Å with an interlayer separation of 3.20 Å.

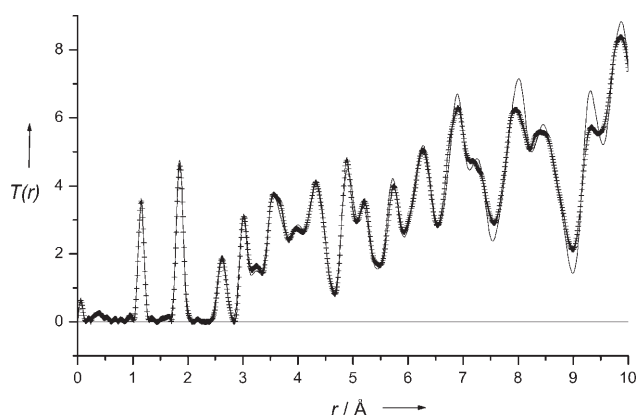


Figure 3. Experimental total pair correlation function in barns \AA^{-2} , $T(r)_{\text{exp}}$ (crosses), and $T(r)_{\text{model}}$ (line) calculated from our model for $\text{Ni}(\text{CN})_2$ at 10 K.

emphasized that this information is directly obtained and independent of the structural model. Remarkably, in the region expected for $\text{Ni}-\text{C}$ and $\text{Ni}-\text{N}$ bonds (1.7–2.3 Å), only one peak is found, showing that both bonds have very similar or identical lengths of approximately 1.86 Å. This result confirms that the assumption of equality made when constructing the structural model was reasonable. The close similarity of $\text{M}-\text{C}$ and $\text{M}-\text{N}$ bonds (to within ca. 0.03 Å), although contrary to naive chemical expectation, has previously been observed in the Group 11 cyanides, CuCN ,^[6] AgCN ,^[11] and AuCN .^[12]

An interesting comparison can be made with the related hydrate, $\text{Ni}(\text{CN})_2 \cdot 3/2 \text{H}_2\text{O}$, the structure of which we have recently determined using powder XRD.^[7] This compound contains layers constructed from linked square-planar $\{\text{Ni}(\text{CN})_4\}$ and octahedrally coordinated $\{\text{Ni}(\text{NC})_4(\text{OH}_2)_2\}$ groups. The $\text{Ni}-\text{C}$ bond (1.866(2) Å) is significantly shorter than and easily distinguishable from the $\text{Ni}-\text{N}$ bond (2.052(2) Å). Two peaks at 1.84 Å and 2.04 Å, corresponding to the $\text{Ni}-\text{C}$ and $\text{Ni}-\text{N}$ bonds, respectively, are clearly visible in $T(r)_{\text{exp}}$ (Figure 4) determined for the deuter-

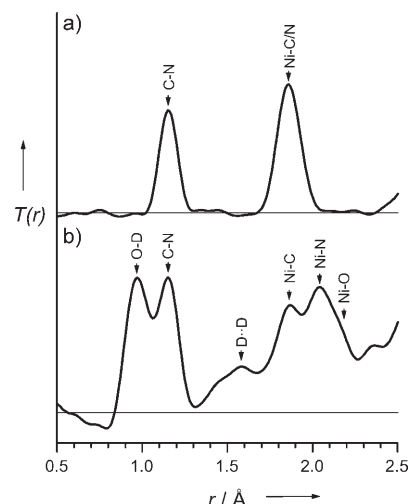


Figure 4. $T(r)_{\text{exp}}$ of a) $\text{Ni}(\text{CN})_2$ and b) $\text{Ni}(\text{CN})_2 \cdot 3/2 \text{D}_2\text{O}$ (0.5–2.5 Å, 300 K). The peaks in the total correlation functions are labeled with the corresponding interatomic distances.

ated analogue, $\text{Ni}(\text{CN})_2 \cdot 3/2 \text{D}_2\text{O}$.^[7] The shoulder on the high r side of the $\text{Ni}-\text{N}$ peak corresponds to the $\text{Ni}-\text{O}$ bond (2.17 Å).

These results suggest that the $\text{C}\equiv\text{N}$ group could be used in molecular switches, as the nitrogen end of the ligand can change its binding characteristics. In $\text{Ni}(\text{CN})_2 \cdot 3/2 \text{H}_2\text{O}$, the nickel atoms in the $\{\text{Ni}(\text{NC})_4(\text{OH}_2)_2\}$ unit are high spin because nitrogen is acting as a weak-field ligand, with the cyanide nitrogen lying between water and ammonia in the spectrochemical series.^[13] Dehydration to $\text{Ni}(\text{CN})_2$ produces low-spin square-planar-coordinated Ni^{2+} ions with a large contraction in the $\text{Ni}-\text{N}$ bond (Figure 5). In addition to the change in interatomic distances, the operation of the switch can also be detected in the change in magnetic properties (paramagnetic to diamagnetic), and as a color change (from pale-blue to yellow). The switch is easily reversible on rehydration, adding to the possible uses of cyanide systems arising from their interesting physical properties.^[14]

A great deal can be determined about the local structure in $\text{Ni}(\text{CN})_2$ by inspection of $T(r)$. However, to confirm that the structural model proposed above is correct, it is necessary to model $T(r)$.^[10] The total pair correlation function, $T(r)_{\text{model}}$, calculated from our structural model for $\text{Ni}(\text{CN})_2$, shows excellent agreement over the range 0–10 Å with the experimentally derived $T(r)_{\text{exp}}$ (Figure 3) confirming that the structure of the sheets and relationship between neighboring sheets have been correctly described. The feature at 3.2 Å

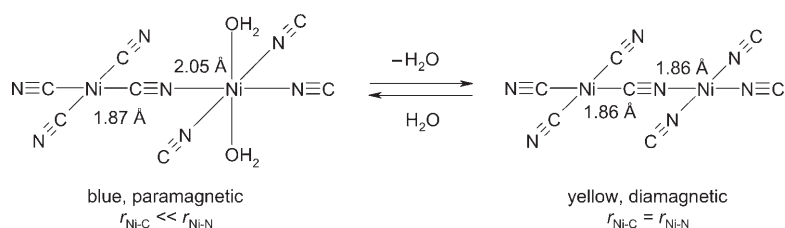


Figure 5. The cyanide group as a reversible molecular switch.

(Figure 3) arises from the relationship between nickel atoms and the nearest-neighbor carbon and nitrogen atoms in adjacent sheets.

Although other models can be formed that replicate the relationship between neighboring sheets, they fail to model $T(r)_{\text{exp}}$ as r increases and cannot account for the observed Bragg reflections, showing that they do not explain the longer range order in the material. Interactions between next-nearest-neighbor layers must also be important in determining the structure of $\text{Ni}(\text{CN})_2$ to produce the stacking sequence ABCBA. However, as in many layer structures, certain stacking faults can form easily because they do not involve a change in nearest-neighbor interactions. The occurrence of a large number of such stacking faults in $\text{Ni}(\text{CN})_2$ explains the broadening of the hkl reflections in the powder XRD pattern.

The behavior of the lattice parameters of $\text{Ni}(\text{CN})_2$ as a function of temperature was determined between 28 and 300 K (Figure 6). Cyanide systems, such as $\text{Zn}(\text{CN})_2$ ^[15,16] and $\text{Cd}(\text{CN})_2$ ^[16] show 3D NTE over similar temperature ranges with relatively large α_l values (-16.9 and $-20.4 \times 10^{-6} \text{ K}^{-1}$, respectively).^[17] $\text{Ni}(\text{CN})_2$ however shows 2D NTE with $\alpha_a = -6.5(1) \times 10^{-6} \text{ K}^{-1}$, a value comparable to those found in the more widely studied oxide systems.^[18] Although the large positive expansion in α_c of $61.8(3) \times 10^{-6} \text{ K}^{-1}$ results in an increase in overall volume with temperature ($\alpha_V = 48.5(4) \times 10^{-6} \text{ K}^{-1}$), this behavior is of interest as it provides a 2D model cyanide system. A number of explanations have been proposed to account for NTE behavior in cyanides, such as rigid-unit modes of linked polyhedra and $\text{M}-\text{C}\equiv\text{N}-\text{M}$ bending motions.^[15,16] Corresponding motions in $\text{Ni}(\text{CN})_2$ include in-plane rotations of the $\{\text{NiC}_4\}$ and $\{\text{NiN}_4\}$ units and rippling of the layers. The large expansion in the c lattice parameter suggests that the latter mode is most important in causing 2D NTE in $\text{Ni}(\text{CN})_2$.

In summary, the dehydration reactions of nickel-cyanide hydrates to produce $\text{Ni}(\text{CN})_2$ show molecular switching behavior in the bonding of the bridging cyanide groups. On dehydration, the nitrogen end of the cyanide ligand changes from a weak-field to a strong-field ligand. This behavior

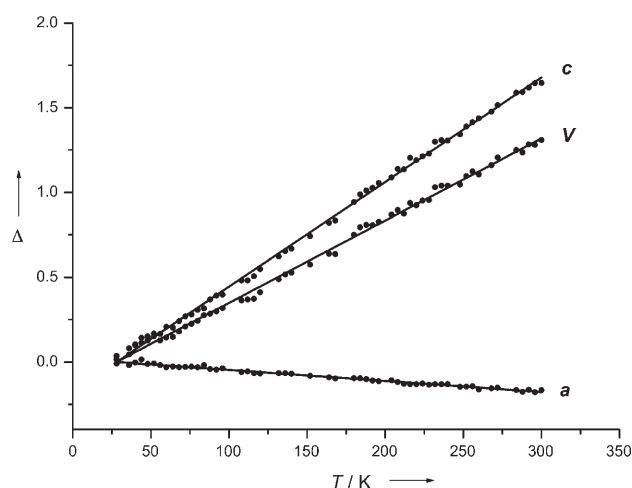


Figure 6. The relative percentage change (Δ) in lattice parameters a and c and cell volume V of $\text{Ni}(\text{CN})_2$ over the range 28–300 K. The straight lines correspond to the least-squares fits.

manifests itself in changes in both the physical and structural properties; in particular, the Ni–C and Ni–N bonds, which differ by approximately 0.2 \AA in the hydrates, become indistinguishable in anhydrous $\text{Ni}(\text{CN})_2$. Remarkably, this is the first reported structure determination of a simple layered cyanide. Similar studies are in progress on $\text{Pd}(\text{CN})_2$ and $\text{Pt}(\text{CN})_2$. In addition to the interest in the structure of $\text{Ni}(\text{CN})_2$ itself, variable-temperature diffraction studies show that it exhibits 2D NTE behavior. Further work will involve determining the atomic mechanism responsible for the NTE behavior and whether the cyanide groups disorder during the dehydration process. Cyanide group order/disorder could not be determined in this neutron diffraction study because of the equality of the Ni–C and Ni–N bond lengths; that is, the very behavior that makes $\text{Ni}(\text{CN})_2$ fascinating.

Received: March 21, 2007

Published online: August 7, 2007

Keywords: cyanides · negative thermal expansion · neutron diffraction · nickel · structure elucidation

- a) K. A. Hofmann, F. Kuespert, *Z. Anorg. Chem.* **1897**, 15, 204; b) H. M. Powell, J. H. Rayner, *Nature* **1949**, 163, 566; c) J. H. Rayner, H. M. Powell, *J. Chem. Soc.* **1952**, 319.
- T. Iwamoto in *Comprehensive Supramolecular Chemistry*, Vol. 6 (Eds.: D. D. MacNicol, F. Toda, R. Bishop), Pergamon, Oxford, **1996**, p. 643.
- G. F. Walker, D. G. Hawthorne, *Trans. Faraday Soc.* **1967**, 63, 166.
- A. Vegas, A. Santos, A. R. Amil, *An. Soc. Esp. Fis. Quim.* **1974**, 70, 214.
- J. L. Manson, W. E. Buschmann, J. S. Miller, *Angew. Chem.* **1998**, 110, 815; *Angew. Chem. Int. Ed.* **1998**, 37, 783.
- S. J. Hibble, S. M. Cheyne, A. C. Hannon, S. G. Eversfield, *Inorg. Chem.* **2002**, 41, 4990.
- For sample preparation and characterization, see the Supporting Information.
- The tetragonal space groups $P4_2$ and $P4_2/mmc$ both produce the same stacking sequence. As neither group allows C/N ordering, the higher symmetry group was selected. Other tetragonal space groups produce incorrect repeat sequences and/or impossibly short atom–atom contacts.
- Neutron diffraction data were collected at 10 and 300 K on the GEM diffractometer, ISIS Facility (see Supporting Information).
- a) S. J. Hibble, A. C. Hannon, I. D. Fawcett, *J. Phys. Condens. Matter* **1999**, 11, 9203; b) S. J. L. Billinge, M. G. Kanatzidis, *Chem. Commun.* **2004**, 749.
- S. J. Hibble, S. M. Cheyne, A. C. Hannon, S. G. Eversfield, *Inorg. Chem.* **2002**, 41, 1042.
- S. J. Hibble, A. C. Hannon, S. M. Cheyne, *Inorg. Chem.* **2003**, 42, 4724.
- A. Ludi, R. Huegi, *Helv. Chim. Acta* **1968**, 51, 349.
- H. Vahrenkamp, A. Geiß, G. N. Richardson, *J. Chem. Soc. Dalton Trans.* **1997**, 3643.
- K. W. Chapman, P. J. Chupas, C. J. Kepert, *J. Am. Chem. Soc.* **2005**, 127, 15630.
- A. L. Goodwin, C. J. Kepert, *Phys. Rev. B* **2005**, 71, 140301.
- The coefficient of thermal expansion α_l for a parameter l is given by $\alpha_l = (l_T - l_0)/l_0(T - T_0)$, where l_T is the parameter l at temperature T and l_0 is the parameter l at T_0 .
- J. S. O. Evans, *J. Chem. Soc. Dalton Trans.* **1999**, 3317.